# Ultrafast thermalization of nonequilibrium holes in p-type tetrahedral semiconductors

Michael Woerner and Thomas Elsaesser
*Max-Born-Institut für Nichtlineare Optik und Kurzzeitspektroskopie, D-12489 Berlin, Germany*
(Received 1 September 1994; revised manuscript received 6 February 1995)

Ultrafast relaxation processes of holes in *p*-type group-IV and -III-V semiconductors are investigated by model calculations. Scattering and energy-loss rates of highly excited nonequilibrium holes are calculated for inter-valence- and intra-valence-band processes with large energy exchange, in particular, optical-phonon scattering and inelastic hole-hole scattering. For both mechanisms of energy loss, the simulation fully takes into account the valence-band dispersion, hole wave functions, and interaction matrix elements of an $8\times8$ $\mathbf{k}\cdot\mathbf{p}$ band-structure calculation and includes dynamical screening of the coupled plasma–optical-phonon system within the random-phase approximation. Inter-valence-band relaxation of split-off holes is dominated by emission of optical phonons via deformation-potential interaction. Inelastic scattering of carriers with the plasma–optical-phonon system represents the main mechanism of hole thermalization. Numerical results are given for *p*-type Ge and GaAs which are compared with femtosecond experiments on hole thermalization.

## I. INTRODUCTION

The nonequilibrium dynamics of free carriers in semiconductors occurs on a subpicosecond time scale and is governed by scattering processes among the carriers and by interaction of electrons and holes with the lattice. Optical studies with ultrashort light pulses give direct insight into these phenomena, allowing the time-resolved observation of the microscopic scattering events.[1] Numerous femtosecond experiments and theoretical simulations have concentrated on the relaxation behavior of photoexcited electron-hole plasma, addressing the coherent generation process of carriers,[2,3] the dynamics of coherent polarizations,[4–6] the redistribution of electrons and holes,[7–10] and carrier cooling.[11] In most cases, the optical response is dominated by electrons and—consequently—there is only limited information on the dynamics of holes that is important from a fundamental physical point of view and relevant for many semiconductor devices.

The investigation of *n*-doped materials with a quasistationary electron distribution gives insight into the hole dynamics. In Refs. 12–14, *n*-doped bulk GaAs and $GaAs/Al_xGa_{1-x}As$ quantum wells have been studied by time-resolved luminescence and time constants of several hundreds of femtoseconds have been reported for hole thermalization, i.e., the relaxation of the photoexcited nonequilibrium carriers to a quasiequilibrium distribution. At low temperature,[12–14] hole-electron scattering was considered the dominant mechanism of thermalization, whereas the very rapid kinetics observed at room temperature was attributed to scattering of holes with optical phonons.[13] The problem of electron-hole interaction can be avoided by investigating a pure hole plasma in *p*-type materials. Very recently, a first femtosecond experiment on the ultrafast relaxation of a pure hole plasma was reported.[15] After excitation of carriers to the split-off (SO) valence band of *p*-type germanium, the redistribution processes were monitored via transient changes of inter-valence-band absorption. Inter-valence-band scattering from the SO to the heavy-hole (HH) and light-hole (LH) valence bands was found to occur within the time resolution of the experiment of 150 fs. The subsequent thermalization of the photoexcited holes proceeds by inelastic hole-hole and hole–optical-phonon scattering with time constants of about 700 fs. The thermalized carriers eventually cool down to lattice temperature by phonon emission within several tens to hundreds of picoseconds. In this paper we present a detailed theoretical analysis of the subpicosecond relaxation behavior of photoexcited holes in bulk GaAs and Ge. The different scattering rates are quantitatively determined with emphasis on inter-valence-band scattering from the SO band and on inelastic carrier-carrier (CC) scattering. In agreement with the experiment, theory predicts a sub-100-fs relaxation time of SO populations. The analysis of CC scattering demonstrates that weak dynamical screening of the long-range Coulomb interaction is essential for the very rapid thermalization kinetics of the carriers. From the carrier dynamics, we calculate the transient optical response of *p*-type germanium that is in quantitative agreement with the data.

The paper is organized in the following way. Starting from a short description of the band-structure model used in the calculations (Sec. II), hole-phonon and hole-plasma scattering rates are calculated in Secs. III A and III B, respectively. Numerical results of the energy relaxation of nonequilibrium holes in *p*-type Ge and GaAs are presented in Sec. IV which are compared with recently published femtosecond experiments on hole thermalization.[15] Conclusions are given in Sec. VI.

## II. BAND STRUCTURE AND HOLE WAVE FUNCTIONS

Two aspects of the valence-band structure are important for the calculation of carrier-carrier and carrier-phonon scattering rates. (i) The energy dispersion of the

 

final band involved in the process determines the density of states to which the particle is scattered. (ii) The overlap of the cell periodic part of the Bloch wave functions of the initial and the final states enters directly into the calculation of the transition-matrix element. In the present calculations, holes with energies in the range of the spin-orbit splitting $\Delta \approx 0.3$ eV and higher ($E_H \leq 0.5$ eV) in Ge or GaAs are considered. The simplest $\mathbf{k}\cdot\mathbf{p}$ theory describing valence-band states in this energy region is given in Ref. 16. There, the $k$-independent spin-orbit interaction as well as the interaction of the lowest conduction band and the upper valence bands are treated exactly whereas the contributions of higher conduction and lower valence bands are taken into account by second-order perturbation theory. With respect to the crystallographic axes, the wave functions are linear combinations of basis functions having the symmetry properties of atomic $S$ and $P$ orbitals under the operations of the tetrahedral group. For the $k$ vector in $z$ direction the doubly degenerate wave functions may be written

$$\begin{aligned}
|i,\alpha,k\rangle &= a_i(k)[iS\downarrow] + b_i(k)[(X-iY)\uparrow/\sqrt{2}] \\
&\quad + c_i(k)[Z\downarrow] , \\
|i,\beta,k\rangle &= a_i(k)[iS\uparrow] - b_i(k)[(X+iY)\downarrow/\sqrt{2}] \\
&\quad + c_i(k)[Z\uparrow] , \\
|\mathrm{HH},\alpha,k\rangle &= [(X+iY)\uparrow/\sqrt{2}] , \\
|\mathrm{HH},\beta,k\rangle &= [(X-iY)\downarrow/\sqrt{2}] ,
\end{aligned} \tag{1}$$

where HH refers to the heavy-hole band and $i$ indexes the light-hole, split-off, and conduction (CB) bands. $a_i$, $b_i$, $c_i$ are functions of $k$ given by Eq. (15) of Ref. 16. For general $k$ direction the wave functions have to be rotated according to Eqs. (6)–(8) of Ref. 16. For any given scattering process from state $|i,\mu,\mathbf{k}\rangle$ to state $|i',\mu',\mathbf{k}'\rangle$ (doubly degenerate spin states are indexed by $\mu,\mu'=\alpha,\beta$) the transition probability depends on the interaction matrix element coupling the various components of the periodic parts [Eq. (1)] of the Bloch functions. For most processes (carrier-carrier, ionized impurity, polar optical, and piezoelectric scattering) the carrier interacts via its charge density with a macroscopic field caused by the third particle involved. In this case the overlap between the periodic parts of the Bloch functions directly enters the matrix element. The corresponding factor $G(i,\mathbf{k},i',\mathbf{k}')$ in the transition probability is defined by[17,18]

$$G(i,\mathbf{k},i',\mathbf{k}') = \tfrac{1}{2} \sum_{\mu,\mu'=\alpha,\beta} |\langle i,\mu,\mathbf{k}|i',\mu',\mathbf{k}'\rangle|^2 . \tag{2}$$

The overlap between the periodic parts is summed over the final spin states $\mu'$ and averaged over initial spin states $\mu$. With isotropic $S$-like wave functions relevant, e.g., for intra-conduction-band scattering close to the $\Gamma$ point (small $\mathbf{k},\mathbf{k}'$), the overlap is unity ($G=1$). For intra-valence-band or interband scattering the $G$ factor depends strongly on the magnitude of $\mathbf{k},\mathbf{k}'$ as well as on the angle between them.

The energy dispersion of the bands is given by the four double roots of the secular equation [Eqs. (9)–(11) of Ref. 16]:

$$E(\mathbf{k}) = k^2 \left\{ \frac{\hbar^2}{2m_e} + M + (L-N-M)W(\theta,\phi) \right\} ,$$

$$W(\theta,\phi) = \frac{k_x^2 k_y^2 + k_y^2 k_z^2 + k_z^2 k_x^2}{k^4} \quad \text{for HH} , \tag{3}$$

$$E'(E'-E_G)(E'+\Delta) - k^2 P^2 (E'+2\Delta/3) = 0 ,$$

$$\begin{aligned}
E_i(\mathbf{k}) = E_i' + k^2 \Bigg\{ & \frac{\hbar^2}{2m_e} + b_i^2 [M + (L-N-M)W(\theta,\phi)] \\
& + c_i^2 \left[ L + \frac{P^2}{E_G} \right. \\
& \left. \left. - 2(L-N-M)W(\theta,\phi) \right] \right\}
\end{aligned}$$

$$\text{for LH, SO, CB} . \tag{4}$$

The band structure is characterized by six parameters, $E_G$, $\Delta$, $P^2$, $L$, $M$, and $N$. The values for Ge and GaAs are listed in Table I.[19] The $\mathbf{k}\cdot\mathbf{p}$ theory at this level of approximation describes the band structure around $k \approx 0$ very well. The HH band shows an approximately parabolic but strongly anisotropic (warped) structure, whereas the LH and SO bands are almost of spherical symmetry with a distinct $k$ dependence of the effective masses (nonparabolic structure). The effective masses of Ge (GaAs) at the band minima resulting from our calculations are (in units of the free electron mass $m_0$): $m_{\mathrm{CB}}=0.036(0.067)$, $m_{\mathrm{SO}}=0.091(0.145)$, $m_{\mathrm{LH}}=0.042(0.074)$, $m_{\mathrm{HH}}(100)=0.21(0.36)$, $m_{\mathrm{HH}}(110)=0.37(0.66)$, and $m_{\mathrm{HH}}(111)=0.49(0.9)$. Obviously, for large values of $k$ (e.g., one-third of the Brillouin zone) the $\mathbf{k}\cdot\mathbf{p}$ theory is less accurate, but nevertheless it can serve as a rough estimate for calculating the final density of states in HH and LH bands in the 0.3-eV region.

## III. SCATTERING PROCESSES

We want to discuss the thermalization of nonequilibrium hole distributions in $p$-type semiconductors following

TABLE I. Ge and GaAs parameters.

| Semiconductor | | Ge | GaAs |
|---|---|---|---|
| Direct energy gap ($T=0$) | $E_G$ (eV) | 0.89 | 1.52 |
| Spin-orbit splitting | $\Delta$ (eV) | 0.29 | 0.34 |
| Conduction-valence band momentum matrix element | $P^2$ (eV $\hbar^2/2m_e$) | 26.8 | 25.7 |
| Valence-band parameter | $L$ ($\hbar^2/2m_e$) | −31.5 | −18.4 |
| Valence-band parameter | $M$ ($\hbar^2/2m_e$) | −5.75 | −3.77 |
| Valence-band parameter | $N$ ($\hbar^2/2m_e$) | −33.9 | −19.6 |
| High-frequency dielectric function | $\epsilon_\infty$ | 16 | 10.91 |
| Frequency LO phonon | $\omega_{\mathrm{LO}}$ (meV) | 37 | 36.5 |
| Frequency TO phonon | $\omega_{\mathrm{TO}}$ (meV) | 37 | 33.8 |
| Optical deformation potential | $d_0$ (eV) | 30 | 30 |

the experimental situation of Ref. 15. In $p$-type material, the holes obey an initial equilibrium distribution from which a nonequilibrium situation is created by femtosecond infrared excitation. The excitation pulse promotes a small fraction of the total carrier density ($\leq 5\%$) to the SO band with an energy separation of several hundreds of meV. The (fast) equilibration of the carriers requires efficient inelastic scattering processes with a distinct loss of excess energy. In contrast, scattering of holes with charged impurities or with acoustic phonons are quasielastic processes contributing only weakly to energy relaxation. However, anisotropic distributions in $k$ space are effectively driven towards isotropic distributions by those elastic mechanisms. Furthermore, the interaction with acoustic phonons represents an additional channel for nearly isoenergetic inter-valence-band transfer of holes.

In $p$-type materials, there are two major scattering mechanisms which dominate the thermalization of nonequilibrium holes: (i) scattering of holes with optical phonons via the deformation potential or the polar interaction, and (ii) carrier-carrier scattering mediated by the long-range Coulomb potential. The combination of high scattering rates with the large amount of energy exchanged in a single scattering process makes both processes much more efficient than any other relaxation channel. Thus the following theoretical treatment of hole thermalization concentrates on these two mechanisms considering carrier distributions isotropic in $k$ space, i.e., the distribution $f_H(E)$ is exclusively a function of the carrier energy $E$.

### A. Optical-phonon scattering via deformation-potential interaction

In tetrahedral semiconductors, such as Ge or GaAs, the carriers couple via the deformation potential to acoustic and optical phonons. The effect of deformation on the hole energy spectrum and the resulting hole-phonon coupling were previously discussed in the limit of valence-band states close to the extremum.[20–22] This procedure was recently extended to the $k$-dependent band structure and hole wave functions presented in the preceding section.[23] In crystals with diamond structure, an optical displacement of both fcc sublattices couples exclusively the subspace of basis functions with $p$ orbital symmetry $|X\rangle$, $|Y\rangle$, $|Z\rangle$ of the same spin. The matrix element for scattering from a hole state $\mathbf{k}$ in the valence band $i$ to the state $\mathbf{k}'=\mathbf{k}+\mathbf{q}$ in the band $i'$ by emission of a single optical phonon with wave vector $\mathbf{q}$ and relative displacement $\mathbf{u}$ can be written as[22,24]

$$M_{ep}=\frac{\sqrt{3}}{2a_0}\langle N_{q,m}+1,i',\mathbf{k}'|\mathbf{D}\cdot\mathbf{u}(b^{\dagger}_{q,m}+b_{q,m})|i,\mathbf{k},N_{q,m}\rangle\ , \tag{5}$$

where $N_{q,m}$ is the phonon occupation number and $b^{\dagger}_{q,m}$, $b_{q,m}$ are the corresponding creation and annihilation operators, respectively. The relative displacement $\mathbf{u}$ can be divided into the amplitude

$$u_0=\sqrt{\hbar V_C/2VM^*\omega_0} \tag{6}$$

and the polarization direction $\mathbf{e}_m$ which can be chosen as $e_x$ or $e_y$ or $e_z$ without loss of generality (in nonpolar semiconductors, such as Ge, the LO and TO phonons are degenerate in the long-wavelength limit). $V_C$ is the volume of the primitive cell, $M^*$ the reduced mass of the atoms contributing to the optical mode with the energy $\hbar\omega_0$, $V$ is the volume of the crystal, and $a_0$ the lattice constant. $\mathbf{D}$ is the deformation-potential operator which can be expressed in representation of the ($|X\rangle,|Y\rangle,|Z\rangle$) basis as [22]

$$\mathbf{D}=d_0\left[\begin{pmatrix}0&0&0\\0&0&1\\0&1&0\end{pmatrix}_x,\begin{pmatrix}0&0&1\\0&0&0\\1&0&0\end{pmatrix}_y,\begin{pmatrix}0&1&0\\1&0&0\\0&0&0\end{pmatrix}_z\right], \tag{7}$$

where $d_0$ is the optical deformation-potential constant. For instance, the basis functions with $|X\rangle$ and $|Y\rangle$ symmetry are coupled via the deformation potential when both fcc sublattices are displaced in $z$ direction. Rates of optical-phonon scattering are calculated in first-order perturbation theory with the help of Fermi's golden rule. The total scattering rate for a hole with the wave vector $\mathbf{k}$ from the valence band $i$ to $i'$ is given by

$$W(i,i',\mathbf{k})=\frac{2\pi}{\hbar}\left[\frac{\sqrt{3}u_0}{2a_0}\right]^2\sum_{\mathbf{k}'}\sum_{m=x,y,z}\sum_{\mu,\mu'=\alpha,\beta}|\langle i',\mu',\mathbf{k}'|D_m e_m|i,\mu,\mathbf{k}\rangle|^2[n(\omega_0)+\tfrac{1}{2}\pm\tfrac{1}{2}]\delta(E_i(\mathbf{k})-E_{i'}(\mathbf{k}')\mp\hbar\omega_0)\ . \tag{8}$$

The rates are averaged over the initial spin states $\mu$ and represent a sum over the final wave vectors $\mathbf{k}'$, final spin states $\mu'$, and polarizations $e_m$ of the phonons involved (upper sign for phonon emission, lower sign for absorption). For a thermal phonon system, the occupation probability $n(\omega_0)$ is the Bose-Einstein factor. For the optical deformation potential $d_0$ of Ge and GaAs similar values have been reported in literature.[19] In our calculations we use a common value of $d_0=30$ eV for both materials which corresponds to $D_0=\sqrt{3/2}(d_0/a_0)=6.3\times10^8$ eV/cm as determined in previous picosecond experiments on carrier cooling in $p$-type Ge.[11] The averaged rates of LO- and TO-phonon emission depend on (i) the density of states in the final band $i'$ and (ii) the symmetry properties of the hole wave functions involved. To illustrate the second point, we consider different scattering processes for initial and final states with symmetry properties at $k=0$, neglecting the different densities of final states. The rates of the following groups of processes: (SO↔LH, SO↔HH), (LH↔LH, LH↔HH, HH↔HH), and (SO↔SO) show a ratio of $1:\frac{1}{2}:0$, respectively. Thus processes depopulating the SO band have

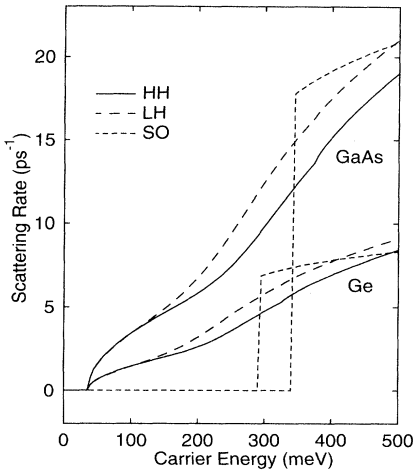


FIG. 1. Scattering rates for holes in GaAs and Ge due to emission of optical phonons via deformation-potential interaction at $T_L=0$ (phonon occupation $N_q=0$). The calculated rates of intravalence and intervalence processes for heavy holes (HH), light holes (LH), and split-off holes (SO) are plotted as a function of the carrier energy.

roughly twice the rates of intraband and interband scattering around the valence-band maximum. Furthermore, there is no optical deformation-potential intraband scattering within the SO band. At larger carrier energies ($E_h \geq 0.3$ eV) the various scattering rates vary in a complicated way depending on the nonparabolic band structure and the $k$-dependent admixture of the basis functions [see Eqs. (1)].

The rates for emission of optical phonons at a lattice temperature of $T_L=0$ [$n(\omega_0)=0$, i.e., no phonon absorption] have been calculated for intra- as well as intervalence-band transitions. The total scattering rates (sum of intraband and interband processes) for heavy holes, light holes, and split-off holes are plotted for Ge and GaAs as a function of carrier energy in Fig. 1. The rates are roughly in the ratio of the density of the final states, $(m_{\mathrm{HH}(110),\mathrm{GaAs}}/m_{\mathrm{HH}(110),\mathrm{Ge}})^{3/2}=2.38$, and show only a weak dependence on the type (HH,LH,SO) of carrier. Optical deformation-potential scattering of SO holes arises exclusively as an inter-valence-band process. It should be noted that the depopulation rate of the SO band due to SO-HH and SO-LH processes at $E_H \approx 400$ meV has a very high value. The corresponding lifetimes of SO holes in GaAs and Ge are 50 and 100 fs, respectively. At higher lattice temperatures these are even shorter due to phonon absorption and other depopulating processes, e.g., acoustic-phonon scattering.

### B. Carrier-carrier and polar-optical scattering

The most efficient process for the thermalization of the nonequilibrium holes is carrier-carrier scattering via the long-range Coulomb interaction. There are several concepts discussed in literature which have been applied to model the equilibration dynamics of plasmas in semiconductors. A commonly used method is the numerical solution of the carrier-carrier Boltzmann equation using a statically screened Coulomb potential.[12,25–27] The effective strength of the Coulomb interaction among the carriers is strongly underestimated in this approximation, resulting—for the present situation—in picosecond equilibration rates of holes that are far too low to account for the observed ultrafast relaxation. An adequate description of hole thermalization requires a weaker dynamical screening of the Coulomb interaction which will be considered in the following. The thermalization dynamics of holes is modeled with the help of a theoretical approach including full dynamic screening. This method was recently applied by Young *et al.* to the scattering of single electrons in an *eh* plasma[28,29] and by Levi and Yafet to the electron transport in bipolar devices[30] including both inelastic Coulomb scattering and polar-optical-phonon scattering.

The treatment is based on the assumption that a given nonequilibrium carrier distribution can be divided into two parts. The first smaller part consists of few excited carriers with high energies, the mutual interaction of which is neglected. The excited holes couple strongly to the major part of the plasma that is assumed to obey a quasiequilibrium statistics characterized by an internal temperature $T_C$ during the whole relaxation process. This concept represents an appropriate description of the transient carrier distributions in the experiments discussed in Ref. 15 where about 3% of the carriers present by doping are excited to the SO band. Inelastic scattering of excited holes with the thermal hole plasma is described in terms of single carriers interacting with fluctuations of the longitudinal macroscopic electric field in the plasma of unexcited carriers at wave vectors $\mathbf{q}$ and frequencies $\omega$. The assumption of thermal equilibrium in the remainder of the plasma allows the application of the dissipation-fluctuation theorem to calculate the inelastic scattering rate $W(i,\mathbf{k})$ for a single carrier in the band $i$ with the wave vector $\mathbf{k}$,

$$W(i,\mathbf{k})=\frac{2\pi}{\hbar}\sum_{i'}\int\frac{d\mathbf{q}}{(2\pi)^3}\frac{4\pi e^2}{q^2}\int_{-\infty}^{\infty}\frac{d\hbar\omega}{\pi}[n(\omega)+1]G(i,\mathbf{k},i',\mathbf{k}+\mathbf{q})[1-f_{i'}(\mathbf{k}+\mathbf{q})]$$
$$\times\mathrm{Im}\left[-\frac{1}{\epsilon(q,\omega)}\right]\delta[E_{i'}(\mathbf{k}+\mathbf{q})-E_i(\mathbf{k})+\hbar\omega]\ . \tag{9}$$

$\epsilon(q,\omega)$ is the longitudinal dielectric response function of the system, $e$ is the electronic charge, $n(\omega)$ is the Bose-Einstein factor, $f_{i'}(\mathbf{k}+\mathbf{q})$ is the distribution function in the final band $i'$, and $G(i,\mathbf{k},i',\mathbf{k}+\mathbf{q})$ is the overlap factor defined in Eq. (2). The scattering rate is summed over the final bands $i'$ and is integrated over all frequencies $\omega$ and

wave vectors $\mathbf{q}$ of the emitted or absorbed (negative frequencies) plasma excitations. In the time-resolved experiment discussed in Ref. 15, the holes are initially excited to very high carrier energies of 400 meV. Here Pauli blocking of the final states is almost completely absent [$f_{i'}(\mathbf{k}+\mathbf{q})\approx 0$]. The calculations show that carrier-plasma scattering strongly favors processes with small momentum transfer ($q \ll k$). Consequently, inter-valence-band scattering via plasma interaction which is connected with a large momentum transfer plays only a negligible role. The plasma scattering of the excited holes is dominated by intraband transitions with an overlap factor close to unity [$G(i,\mathbf{k},i,\mathbf{k}+\mathbf{q})\approx 1$ for $\mathbf{k}+\mathbf{q}\approx\mathbf{k}$].

The longitudinal dielectric response function $\epsilon(q,\omega)$ is calculated in the random phase approximation (RPA) considering intra- as well as inter-valence-band transitions.[31] In the most general form we will consider

$$\epsilon(q,\omega)=\epsilon_\infty-4\pi\left[\chi_L(\omega)+\sum_{i,i'}\chi_{i,i'}(q,\omega)\right] . \tag{10}$$

Here $\epsilon_\infty$ is the high-frequency limit of the dielectric response function. $\chi_L(\omega)$ is the frequency-dependent lattice susceptibility

$$\chi_L(\omega)=\frac{\epsilon_\infty(\omega_{\mathrm{TO}}^2-\omega_{\mathrm{LO}}^2)}{4\pi(\omega_{\mathrm{TO}}^2-\omega^2)} , \tag{11}$$

where $\omega_{\mathrm{LO}}$ and $\omega_{\mathrm{TO}}$ are the longitudinal- and transverse-optical-phonon frequencies, respectively. In polar materials, i.e., III-V and II-VI compounds, this term causes an additional coupling between the carriers and LO phonons resulting in the well-known polar-optical-phonon scattering. In the case of group-IV semiconductors, e.g., germanium, the TO- and LO-phonon frequencies are identical and the lattice susceptibility [Eq. (11)] vanishes. $\chi_{i,i'}(q,\omega)$ in Eq. (10) are the various intra- and inter-valence-band susceptibilities, the imaginary parts of which are calculated with[28]

$$\begin{aligned}\mathrm{Im}[\chi_{i,i'}(q,\omega)]=-\frac{2\pi e^2}{q^2}\int\frac{d\mathbf{k}}{(2\pi)^3}G(i,\mathbf{k},i',\mathbf{k}+\mathbf{q})\\ \times[f_i(\mathbf{k})-f_{i'}(\mathbf{k}+\mathbf{q})]\\ \times\delta[E_i(\mathbf{k})-E_{i'}(\mathbf{k}+\mathbf{q})+\hbar\omega] ,\end{aligned} \tag{12}$$

with the hole distribution function $f_i(\mathbf{k})$ in the valence band $i$ and the corresponding carrier energies $E_i(\mathbf{k})$. Finally, the real part of the susceptibilities $\chi(q,\omega)$ is obtained from integrating the imaginary parts numerically (using the Kramers-Kronig relations). For our simulation of hole thermalization in $p$-type Ge we use the approximation of low excitation ($p_{\mathrm{ex}} \ll p_0$), i.e., only the contribution of the unexcited holes which are the major part of the plasma is regarded for the calculation of the dielectric response function $\epsilon(q,\omega)$. These holes are concentrated at energies around the valence-band maximum. Thus it is a good approximation to include only the intraband and interband susceptibilities of the heavy-hole and light-hole valence bands [$i,i'$=HH,LH in Eq. (12)] in the calculation of $\epsilon(q,\omega)$ [Eq. (10)]. For low excitation densities $p_{\mathrm{ex}} \ll p_0$, a weak transient spectral hole in HH distribution caused by the excitation process is leveled out on a sub-100-fs time scale by ultrafast intraband thermalization among the heavy holes. This fact is confirmed by experimental[15] and theoretical results[32] where the relaxation of spectral holes in a dense carrier distribution with very high collision frequencies has been simulated in detailed theoretical calculations including a dynamically screened Coulomb interaction. Thus the unexcited heavy and light holes obey a common Fermi distribution function $f_H(E)$ during the excitation and the subsequent relaxation process. The Fermi level $\mu$ and the momentary carrier temperature $T_C$ are related to the carrier density $p_0$, which is constant in our simulation (and the experiment discussed in Ref. 15):

$$p_0=\int_0^\infty dE\, D(E) f_H(E) . \tag{13}$$

$D(E)$ is the combined density of states of the HH and LH bands. Now, the rate of inelastic plasma scattering $W(i,E_i(\mathbf{k}))$ can be calculated for a hole in the valence band $i$ as a function of the carrier energy $E_i(\mathbf{k})$ with help of Eq. (9) for a plasma of unexcited holes characterized by the longitudinal dielectric response function $\epsilon(q,\omega)$ [Eq. (10)] which depends in the case of nonpolar materials on two parameters, the plasma density $p_0$ and the carrier temperature $T_C$. The corresponding energy-loss rate $P(i,E_i(\mathbf{k}))$ is gained by multiplying the integrand of Eq. (9) with the energy $\hbar\omega_{\mathrm{pl}}$ of the plasma excitations. The average energy loss per scattering event is given by $P(i,E_i(\mathbf{k}))/W(i,E_i(\mathbf{k}))$.

### C. Carrier-plasma scattering in $p$-type Ge

In Fig. 2(a), the total scattering rates of excited carriers in the HH (solid line), the LH (short-dashed line), and the SO bands (dashed line) of Ge are plotted versus their excess energy for a total carrier concentration of $p_0=3\times10^{17}$ cm$^{-3}$ and a carrier temperature of $T_C=0$. The rates, which depend slightly on the effective mass of the holes, show a steep rise up to carrier energies of $E_H\approx 50$ meV and level off at higher $E_H$. A detailed analysis of the hole-plasma interaction shows that the rates are dominated by HH to LH *inter-valence-band* transitions in the cold plasma which strongly enhance small angle scattering. It should be noted that the total scattering rate of excited holes at low and medium excess energies is dominated by the hole-plasma interaction whereas hole–optical-phonon processes make a significant contribution for $E_H > 0.5$ eV.

The average energy loss per collision and energy-loss rate due to inelastic hole-hole scattering are shown in Figs. 2(b) and 2(c), respectively. For the plasma density considered here, the energy emitted per scattering event is comparable with the optical-phonon energy of Ge, i.e., the higher rate of hole-hole scattering results in an energy-loss rate via inelastic plasma scattering significantly higher than by emission of optical phonons.

In Fig. 3, the scattering rates are plotted for a wide range of carrier densities. The total scattering rate (a)

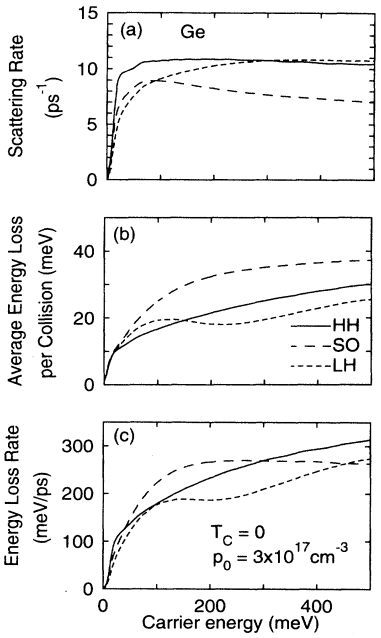


FIG. 2. Inelastic scattering of holes with plasma excitations in $p$-type germanium for a thermal hole plasma of a density of $p_0=3\times10^{17}$ cm$^{-3}$ and a carrier temperature of $T_C=0$. (a) Calculated scattering rates for HH (solid lines), SO (long-dashed lines), and LH (short-dashed lines) as a function of the carrier energy. (b) Average energy loss per inelastic scattering event. (c) Calculated energy-loss rates of plasma scattering.

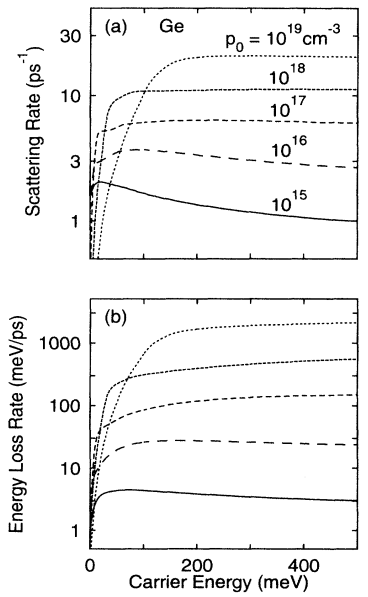


FIG. 3. Calculated HH scattering rates for hole plasmas with various densities of $p_0=10^{15}$, $10^{16}$, $10^{17}$, $10^{18}$, and $10^{19}$ cm$^{-3}$ at a carrier temperature of $T_C=0$. The scattering rates (a) and energy-loss rates (b) are plotted on a logarithmic scale vs the carrier energy.

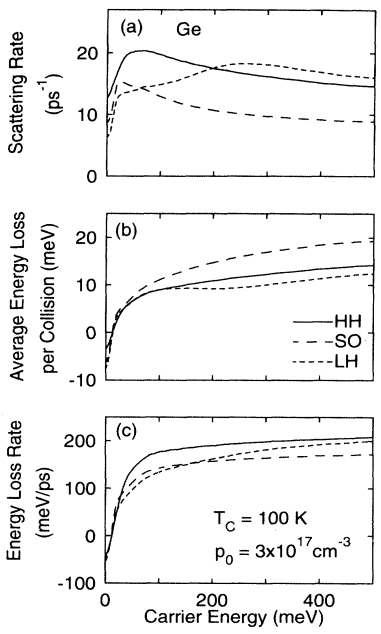


FIG. 4. Calculated scattering and energy-loss rates for a hole plasma with $p_0=3\times10^{17}$ cm$^{-3}$ and a carrier temperature of $T_C=100$ K (plotted as in Fig. 2).

and the energy-loss rate (b) are plotted on a logarithmic scale versus the hole energy for plasma densities of $p_0=10^{15}$, $10^{16}$, $10^{17}$, $10^{18}$, and $10^{19}$ cm$^{-3}$ at a carrier temperature of $T_C=10$ K. The rates for holes at small carrier energies are lowered for the higher plasma densities. At high carrier energies ($E_H\approx400$ meV), the scattering rates show a relatively weak, sublinear change with carrier densities. For a change of carrier concentration by four orders of magnitude (from $p_0=10^{15}$ to $10^{19}$ cm$^{-3}$), the total scattering rate [Fig. 3(a)] varies by only a factor of 20 whereas the energy-loss rate [Fig. 2(b)] changes by a factor of 500. This insensitivity of the inelastic carrier-carrier scattering rate to the plasma density is caused by the very effective screening of the Coulomb interaction at high carrier concentrations.

The theoretical curves in Fig. 4 were calculated with the same parameters as the results of Fig. 2, but for a plasma temperature of $T_C=100$ K. In comparison to Fig. 2, we observe higher scattering rates but lower energy-loss rates and, consequently, a lower average energy loss per scattering event. The reduced energy loss is due to absorption of plasma excitations, which increases the total scattering rate [Fig. 4(a)] and leads to a flow of energy to the highly excited carriers.

### D. Scattering of holes with the coupled plasma–optical-phonon system in $p$-type GaAs

In the case of polar semiconductors like GaAs, the interaction of carriers with the plasma is more complicated. The longitudinal dielectric response function [Eq. (10)] contains an additional term due to the lattice susceptibili-

ty [Eq. (11)]. This term causes polar coupling between the carriers and longitudinal-optical phonons. In the presence of both plasma and lattice, there are coupled modes of the plasma–optical-phonon system and the interaction of carriers with one part of this system is influenced by the other part due to screening or antiscreening. To separate the various contributions to the total scattering rate of holes in $p$-type GaAs the loss function $\mathrm{Im}[1/\epsilon(\omega,q)]$ in the integrand of Eq. (9) can be divided into additive terms:

$$\mathrm{Im}\left[-\frac{1}{\epsilon(q,\omega)}\right]=\sum_i \frac{4\pi\,\mathrm{Im}\chi_i(\omega,q)}{|\epsilon(\omega,q)|^2}\ . \tag{14}$$

$\chi_i(\omega,q)$ are the various susceptibilities of the lattice [Eq. (11)] and intra- and inter-valence-band excitations [Eq. (12)] whereas $\epsilon(\omega,q)$ [Eq. (10)] is the dielectric function of the entire plasma–optical-phonon system. After integrating the various additive terms separately we get the following results for hole scattering in $p$-type GaAs. In Fig. 5(a) inelastic scattering of heavy holes with excitations of the coupled plasma–optical-phonon system in $p$-type GaAs is shown for a plasma density of $p_0=3\times10^{17}$ cm$^{-3}$ and a temperature of $T_C=T_L=0$. The solid line represents the total rate of coupled plasma–optical-phonon scattering for heavy holes as a function of the carrier energy. The various contributions [Eq. (14)] to this rate are emission of LO phonons via the polar interaction (long-dashed line) and excitation of plasma modes due to inter- (medium-dashed line) and intra-valence-band transitions (short-dashed line). The corresponding energy-loss rate for HH scattering is depicted in Fig. 5(b). In contrast to the nonpolar semiconductor Ge, the total scattering and energy-loss rate due to optical-phonon emission, polar plus nonpolar (see Fig. 1), is much higher than the rate of carrier-plasma scattering. Again, the inter-valence-band excitations (medium-dashed line) in the hole plasma play the dominant role for the latter process. This different behavior is caused by the higher density of final states for optical deformation-potential scattering (Fig. 1) and by the additional coupling to LO phonons due to the presence of ionicity in GaAs.

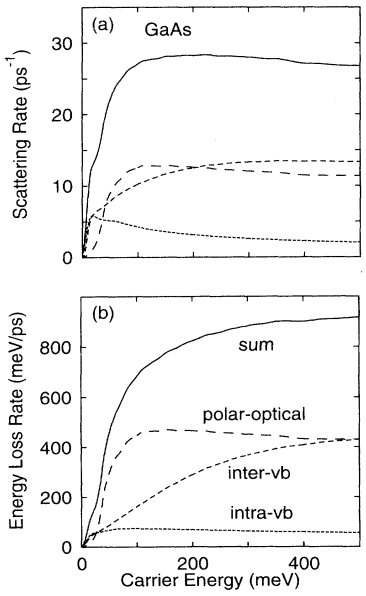


FIG. 5. Inelastic scattering of holes with excitations of the coupled plasma–optical-phonon system in $p$-type GaAs for a plasma density of $p_0=3\times10^{17}$ cm$^{-3}$ and a temperature of $T_C=T_L=0$. (a) Various contributions to the total rate (solid line) of coupled plasma–optical-phonon scattering for heavy holes as a function of the carrier energy. Long-dashed line: polar-optical-phonon part; medium-dashed line: plasma inter-valence-band excitations; short-dashed line: plasma intra-valence-band excitations. (c) Corresponding energy-loss rates for HH scattering.

## IV. ENERGY RELAXATION OF NONEQUILIBRIUM HOLES

### A. Hole relaxation in $p$-type Ge

In this section, we compare our numerical results with recently published femtosecond experiments which provide specific insight into the ultrafast thermalization process of a single-component hole plasma in $p$-type germanium.[15] A 200-$\mu$m-thick crystal with a doping concentration of $N_A=3\times10^{17}$ cm$^{-3}$ was investigated. In the time-resolved experiments, an intense infrared pulse of 300 fs duration excites about 5% of the holes from the HH to the SO valence band. The resulting absorption change of the HH to SO transition is monitored by weak probe pulses at various wavelengths and gives information on the femtosecond hole relaxation. The time resolution was 150 fs.

The essential experimental results are the following. (i) The holes excited to the SO band scatter back to the LH and HH bands within the time resolution of the experiment. This experimental fact is supported by the numerical results of this paper. The calculation of the inter-valence-band scattering rate by optical-phonon emission in Ge (see Fig. 1) provides a lifetime for carriers in the split-off band of roughly $\tau_{\mathrm{life}}^{\mathrm{SO}}\approx120$ fs $=[W_{\mathrm{phonon}}(\mathrm{SO}\rightarrow\mathrm{HH})+W_{\mathrm{phonon}}(\mathrm{SO}\rightarrow\mathrm{LH})]^{-1}$. The high density of final states in the HH and LH bands favors the very rapid depopulation of the SO band. (ii) After inter-valence-band scattering, the hole distribution still has a distinct nonequilibrium character. The major part of the plasma, the unexcited holes, occupies states of small energy around $k=0$ with a quasiequilibrium distribution function. The small fraction of excited holes populates states in the HH and LH bands at high energies in the range of $E_H\approx400$ meV. These carriers lose their excess energy by (i) emission of phonons and (ii) inelastic carrier-carrier scattering. Emission of optical phonons via the deformation potential makes the main contribution to the first mechanism. In Fig. 1, the corresponding calculated scattering rates are plotted as a function of the carrier energy. In the range of $E_H\approx400$ meV the holes emit roughly seven optical phonons per picosecond. The second process, i.e., inelastic Coulomb scattering with the

cold plasma of unexcited holes, results in an equilibration of the hole distribution. The rise time of the transient absorption of about 700 fs in the experiment of Ref. 15 is directly related to the energy transfer from the photoexcited hot carriers to the cold plasma of unexcited holes. For a quantitative comparison of theory and experiment, we calculate the energy relaxation of nonequilibrium holes from the following coupled differential equations for the transient carrier temperature $T_C(t)$, and for the momentary energy of the initially excited holes $E_H^{\rm ex}(t)$:

$$\frac{dE_H^{\rm ex}}{dt} = -\frac{dE[\rightarrow(\text{lattice})]}{dt} - \frac{dE[\rightarrow(\text{plasma})]}{dt} , \tag{15}$$

$$\frac{dE[\rightarrow(\text{lattice})]}{dt} = \hbar\omega_0[W^{\rm em}_{\rm phonon}(T_L,E_H^{\rm ex}) - W^{\rm abs}_{\rm phonon}(T_L,E_H^{\rm ex})] , \tag{16}$$

$$\frac{dE[\rightarrow(\text{plasma})]}{dt} = P^{\rm loss}_{\rm plasma}(T_C,E_H^{\rm ex}) , \tag{17}$$

$$\frac{d\langle E(T_C)\rangle}{dt} = \left[\frac{p_{\rm ex}}{p_0-p_{\rm ex}}\right]\frac{dE[\rightarrow(\text{plasma})]}{dt} . \tag{18}$$

Equation (15) describes the energy loss of the initially excited carriers and Eqs. (16) and (17) consider the energy transfer of the high-energy holes to the lattice and to the plasma of unexcited holes (density $p_0$), respectively. The fraction of excited carriers $p_{\rm ex}/p_0$ determines the transient plasma temperature $T_C(t)$ which is directly connected with the average carrier energy in the remainder of the plasma $\langle E(T_C)\rangle$ [Eq. (18)]. For low excitation densities ($p_{\rm ex} \ll p_0$) the energy relaxation of the excited holes $E_H^{\rm ex}(t)$ is almost independent of $p_{\rm ex}$. Using the parameters of the time-resolved experiment,[15] $p_0 = 3\times10^{17}$ cm$^{-3}$, $T_C(t=0) = T_L = 10$ K, $p_{\rm ex}(t=0) = 10^{16}$ cm$^{-3}$, the energy relaxation of nonequilibrium holes initially excited to $E_H^{\rm ex}(t=0) = 500$ meV has been calculated and is shown in Fig. 6(a). The temporal evolution of the carrier energy $E_H^{\rm ex}(t)$ (solid line) and the energies fractionally transferred to the plasma $E(\rightarrow\text{lattice})$ (long-dashed line) and to the lattice $E(\rightarrow\text{plasma})$ (short-dashed line) are plotted versus time in picoseconds. We observe an approximately exponential rise of $E(\rightarrow\text{plasma})$ with a time constant of $\tau_{\rm rise} \approx 800$ fs. The final value of $E(\rightarrow\text{plasma}, t=2\text{ ps}) = 340$ meV corresponds to a plasma temperature of $T_C = 80$ K. This is in very good agreement with the experimental results of Ref. 15 and thus confirms our physical picture of the thermalization process. For the given density $p_0$ the main part of the excess energy flows to the plasma of unexcited holes, resulting in an elevated carrier temperature $T_C$. The simulations show that the weak *dynamical* screening of the Coulomb interaction [frequency dependence of the dielectric response function $\varepsilon(q,\omega)$] and the HH to LH *inter-valence-band* transitions in the cold plasma play the major role for the rapid energy loss of the high-energy carriers.

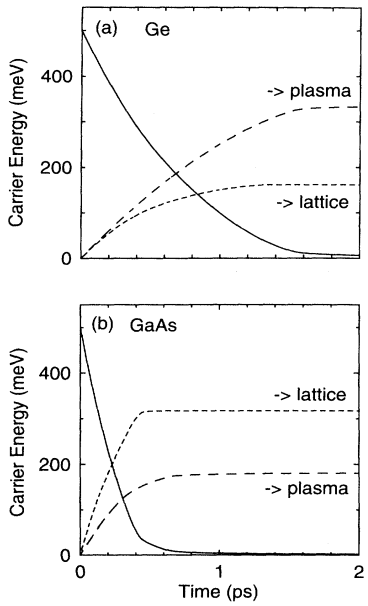


FIG. 6. (a) Transient energy loss of holes excited to HH states with $E_{\rm HH} = 500$ meV in $p$-type Ge with a hole density of $p_0 = 3\times10^{17}$ cm$^{-3}$ at $T_C = T_L = 0$. The transient energy of the relaxing carriers (solid line) is plotted vs time in picoseconds. The transferred energies to the cold hole plasma of unexcited holes and to the lattice via optical-phonon emission are shown as long- and short-dashed lines, respectively. (b) Transient energy loss of heavy holes in $p$-type GaAs [parameters and plot as in (a)].

### B. Energy relaxation of holes in $p$-type GaAs

For comparison we simulated the energy relaxation of nonequilibrium holes in $p$-type GaAs under the same conditions as for Ge discussed in the preceding section. The results are presented in Fig. 6(b). In contrast to $p$-type Ge, the relaxation in $p$-type GaAs is much faster. After fitting an exponential decay curve to the data (solid line) we deduce a time constant of $\tau_E = 300$ fs for the energy relaxation. This enhanced dissipation is mainly due to the more pronounced polar- as well as nonpolar-phonon scattering in GaAs (cf. Figs. 1 and 5). At this plasma density the excited carriers transfer the major part of their energy to the lattice [short-dashed line in Fig. 6(b)]. The reversed situation as in Ge [see Fig. 6(a)] is attained for hole plasmas with much higher density where the optical-phonon scattering is reduced by screening of the polar interaction and the carrier-plasma scattering is enhanced due to the higher density.

## V. CONCLUSIONS

In conclusion, the theoretical results presented here give evidence that the relaxation of nonequilibrium holes in $p$-type tetrahedral semiconductors happens on an ultrafast subpicosecond time scale. Theoretical studies on $p$-type Ge and GaAs reveal that the lifetime of holes in the SO valence bands is 100 and 50 fs, respectively, due to

very rapid inter-valence-band scattering via the optical deformation potential. The equilibration of excited holes with the remainder of the plasma at excess energies of several hundreds of meV occurs with time constants of about 300–700 fs. Nonpolar materials show a stronger coupling to the hole plasma whereas the presence of ionicity in III-V components favors the energy transfer to the lattice. The very good agreement of the theoretical results with a recently published experiment on hole thermalization in Ge confirms our detailed physical picture of the ultrafast thermalization of nonequilibrium holes in *p*-type semiconductors.


[1]See, e.g., *Proceedings of the 8th International Conference on Hot Carriers in Semiconductors,* edited by J. F. Ryan and A. C. Maciel [Semicond. Sci. Technol. **9**, Number 5S (1994)].

[2]F. Rossi, S. Haas, and T. Kuhn, Phys. Rev. Lett. **72**, 152 (1994).

[3]A. Leitenstorfer, A. Lohner, T. Elsaesser, S. Haas, F. Rossi, T. Kuhn, W. Klein, G. Boehm, G. Traenkle, and G. Weimann, Phys. Rev. Lett. **73**, 1687 (1994).

[4]D. S. Kim, J. Shah, T. C. Damen, W. Schäfer, F. Jahnke, S. Schmitt-Rink, and K. Köhler, Phys. Rev. Lett. **69**, 2725 (1992).

[5]S. Weiss, M.-A. Mycek, J.-Y. Bigot, S. Schmitt-Rink, and D. S. Chemla, Phys. Rev. Lett. **69**, 2685 (1992).

[6]M. Koch, J. Feldmann, G. von Plessen, E. O. Göbel, P. Thomas, and K. Köhler, Phys. Rev. Lett. **69**, 3631 (1992).

[7]W. Z. Lin, R. W. Schoenlein, J. G. Fujimoto, and E. P. Ippen, IEEE J. Quantum Electron. **24**, 267 (1988).

[8]W. H. Knox, C. Hirlimann, D. A. B. Miller, J. Shah, D. S. Chemla, and C. V. Shank, Phys. Rev. Lett. **56**, 1191 (1986).

[9]T. Elsaesser, J. Shah, L. Rota, and P. Lugli, Phys. Rev. Lett. **66**, 1757 (1991).

[10]L. Rota, P. Lugli, T. Elsaesser, and J. Shah, Phys. Rev. B **47**, 4226 (1993).

[11]M. Woerner, T. Elsaesser, and W. Kaiser, Phys. Rev. B **45**, 8378 (1992).

[12]A. Chebira, J. Chesnoy, and G. M. Gale, Phys. Rev. B **46**, 4559 (1992).

[13]X. Q. Zhou, K. Leo, and H. Kurz, Phys. Rev. B **45**, 3886 (1992).

[14]A. Tomita, J. Shah, J. E. Cunningham, S. M. Goodnick, P. Lugli, and S. L. Chuang, Phys. Rev. B **48**, 5708 (1993).

[15]M. Woerner, W. Frey, M. T. Portella, C. Ludwig, T. Elsaesser, and W. Kaiser, Phys. Rev. B **49**, 17 007 (1994).

[16]E. O. Kane, J. Phys. Chem. Solids **1**, 249 (1957).

[17]M. O. Vassell, A. K. Ganguly, and E. M. Conwell, Phys. Rev. B **2**, 948 (1970).

[18]J. D. Wiley, Phys. Rev. B **4**, 2485 (1971).

[19]*Semiconductors, Physics of Group IV Elements and III-V Compounds,* edited by K.-H. Hellwege and O. Madelung, Landolt-Börnstein, New Series, Group III, Vol. 17, Pt. a (Springer-Verlag, Berlin, 1982).

[20]G. L. Bir and G. E. Pikus, Fiz. Tverd. Tela (Leningrad) **2**, 2287 (1960) [Sov. Phys. Solid State **2**, 2039 (1961)].

[21]P. Lawaetz, Phys. Rev. **174**, 867 (1968).

[22]A. Cantarero, C. Trallero-Giner, and M. Cardona, Phys. Rev. B **39**, 8388 (1989).

[23]R. Scholz, J. Appl. Phys. **77**, 3219 (1995).

[24]W. Poetz and P. Vogl, Phys. Rev. B **24**, 2025 (1981).

[25]D. Pines, Phys. Rev. **92**, 626 (1953).

[26]C. J. Hearn, Proc. Phys. Soc. London **86**, 881 (1965).

[27]D. W. Snoke, W. W. Ruehle, Y. C. Lu, and E. Bauser, Phys. Rev. B **45**, 10 979 (1992).

[28]J. F. Young, N. L. Henry, and P. J. Kelly, Solid-State Electron. **32**, 1567 (1989).

[29]J. F. Young and P. J. Kelly, Phys. Rev. B **47**, 6316 (1993).

[30]A. F. J. Levi and Y. Yafet, Appl. Phys. Lett. **51**, 42 (1987).

[31]W. Bardyszewski, Solid State Commun. **57**, 873 (1986).

[32]R. Binder, D. Scott, A. E. Paul, M. Lindberg, K. Henneberger, and S. W. Koch, Phys. Rev. B **45**, 1107 (1992).